Pramana – J. Phys. (2021) 95:82
https://doi.org/10.1007/s12043-021-02121-0

Antibunching of photons in a coherent radiation field coupled to a non-degenerate parametric oscillator beyond rotating wave approximation

SWAPAN MANDAL[1],*, MOHOSIN ALAM[1], MONOJIT KORA[1] and MOHAMED RIDZA WAHIDDIN[2]

[1]Department of Physics, Visva Bharati, Santiniketan 731 235, India
[2]Department of Computer Science, Kulliyyah of ICT, International Islamic University Malaysia, 53100 Kuala Lumpur, Malaysia
*Corresponding author. E-mail: swapanvb@rediffmail.com

MS received 23 July 2020; revised 16 January 2021; accepted 27 January 2021

Abstract. Under the classical (strong) pump condition, the Hamiltonian involving the signal and the idler modes of a non-degenerate parametric oscillator is exhibited. Without using the usual rotating wave approximation (RWA), the analytical solutions of the field operators are used to investigate the antibunching of photons of the input radiation field coupled to the non-degenerate parametric oscillator. By using the symbolic calculation, the antibunching of photons for both the signal and idler modes are investigated. In particular, the effects of the inclusion of rotating wave approximated terms on the antibunching of photons are clearly indicated. To substantiate the analytical results, the temporal evolution of signal photon and idler photons, and the antibunching effects of the signal and idler modes are investigated numerically by using the QuTip 3.1.0. The exact numerical results obtained by QuTip 3.1.0 matches extremely well with those of the analytical results. The present article and hence the analytical method might be of use for investigating the situations of having ultra-strongly and deep-strongly coupled systems where the possibilities of using RWA is completely ruled out.

Keywords. Antibunching of photons; non-degenerate parametric oscillators; rotating wave approximation.

PACS Nos 42.50.−p; 42.50.Ct; 42.50.Pq

1. Introduction

The interaction of the electromagnetic field with the material medium is of fundamental interest. The electromagnetic field induces polarisation in the material medium. The induced polarisation proportional to the amplitude of the electromagnetic field is said to be a linear one. The linear polarisation arises as long as the intensity of the applied electromagnetic field is not too high. The linear nature of polarisation and hence the linear optical regime is sufficient to explain the usual phenomena of reflection and refraction. The importance of linear polarisation regime prevailed till the discovery of the laser. The availability of strong electromagnetic fields through a laser source has made a remarkable change in the concept of polarisation. With the availability of high power laser sources, the concept of nonlinear polarisation and hence the nonlinear susceptibility has become a reality. The first and foremost nonlinear polarisation in a medium is contributed by the second-order one. The second-order nonlinear medium interacting with an external electromagnetic field produces second harmonic generation, parametric interaction, and the sum- and difference-frequency generation [1–6]. The maiden observation of second harmonic generation was reported by Franken *et al* [6]. The parametric interaction is also an important phenomenon of the matter–field interaction involving second-order nonlinear susceptibility. In a parametric interaction, a strong pump of frequency Ω_3 interacts with a second-order nonlinear medium and produces a signal photon and idler photon of frequencies Ω_1 and Ω_2 respectively. The parametric interaction taking place in a resonant cavity is termed as the parametric oscillator. The quantum statistical properties of the radiation fields coupled to the parametric oscillator are well investigated [7–13]. In the parametric interaction, the conservation of energy is respected and hence $\Omega_3 = \Omega_1 + \Omega_2$. For

Published online: 15 May 2021

$\Omega_1 \neq \Omega_2$, the corresponding parametric oscillator is termed as a non-degenerate one. We observe that most of the nonlinear matter–field interactions are investigated under the subject of nonlinear optics and hence in the classical regime. On the other hand, the relatively lower intensity in a particular mode demands the consideration of the quantisation of the electromagnetic field and hence the quantum optical treatment. In the present investigation, we consider the quantised versions of the signal and the idler fields. The presence of nonlinearity and hence the nonlinear terms in the interaction Hamiltonian make the problem unsolvable in a closed analytical form unless rotating wave approximation (RWA) is used. The essence of RWA is to eliminate the fast rotating terms and hence to obtain a relatively easier form of equations of motion involving the field operators. The application of RWA is certainly useful and is widely accepted for solving the atom–field interaction in a much easier way. On the other hand, we know that the cost of using the RWA is extremely heavy in the low-frequency region. For example, the Bloch–Siegert shift is basically the outcome of the inclusion of terms which are normally neglected during the RWA [14]. It is established that the use of RWA leads to incorrect results for investigating Berry's phase [15]. The significant departures in Rabi oscillations in two-photon Jaynes–Cummings model beyond RWA compared to its RWA counterpart are exhibited by using multiscale perturbation theory [16]. In the context of atom–field entanglement, it is established that the use of RWA is not necessary for dealing with the Jaynes–Cummings model [17]. The necessity of going beyond the RWA is found necessary when we consider the ultra-strongly and deep-strongly coupled systems [18–23]. Keeping these points in mind, we investigate the effects of the inclusion of terms which are usually neglected under RWA for making the problems easier to solve. In this way, the present analytical approach towards the problem of non-degenerate parametric oscillator (NDPO) enjoys the maiden one status where the RWA is not used. The solutions to the NDPO beyond the RWA are used to investigate the non-classical properties of the thermal and coherent light coupled to the said NDPO. These non-classical properties include squeezing and antibunching of photons.

The paper is organised as follows: The model Hamiltonian and hence the solution of the NDPO beyond the RWA is discussed in §2. In §3, we give some useful expressions for the temporal evolution of operators. Before we conclude in §5, we discuss the effects of non-synchronous terms on photon antibunching of the input radiation fields prepared in coherent state and in number states (§4).

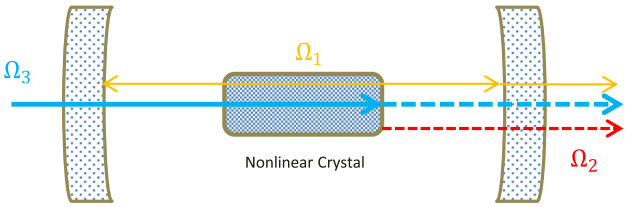

Figure 1. Schematic diagram of non-degenerate parametric oscillator with pump frequency $\Omega_3 = \Omega_1 + \Omega_2$, where Ω_1 and Ω_2 are the signal and idler frequencies respectively.

2. Model Hamiltonian of non-degenerate parametric oscillator

The model Hamiltonian of a non-degenerate parametric oscillator (NDPO) with pump frequency Ω_3 and coupling strength g follows as [2,24]

$$H = \hbar\Omega_1\left(a_1^\dagger a_1 + \frac{1}{2}\right) + \hbar\Omega_2\left(a_2^\dagger a_2 + \frac{1}{2}\right) + 2g\hbar\cos\Omega_3 t\,(a_1^\dagger - a_1)(a_2^\dagger - a_2), \quad (1)$$

where $a_1(a_2)$ and $a_1^\dagger(a_2^\dagger)$ are termed as the annihilation and creation operators of the signal (idler) field respectively. The schematic diagram (figure 1) shows that the frequency of strong classical pump is $\Omega_3 = \Omega_1 + \Omega_2$ and is responsible for the generation of signal and idler waves of Ω_1 and Ω_2 respectively. The coupling parameter g appearing in eq. (1) involves the pump amplitude and the second-order nonlinear susceptibility. Now, we have the following commutation relations:

$$[a_i, a_j^\dagger] = \delta_{ij}, \quad [a_i, a_j] = 0 \quad \text{and} \quad [a_i^\dagger, a_j^\dagger] = 0. \quad (2)$$

In order to investigate non-classical properties of the radiation field and hence the antibunching of photons, we have to obtain the solution of the Hamiltonian (1). In order to do so, the Heisenberg operator equations of motion involving a_1 and a_2 are to be obtained. It is found that these differential equations are coupled to each other. Nevertheless, the differential equations involve variable coefficients. In order to obtain analytical solutions to the coupled differential equations, we propose the following solutions [24,25]:

$$a_1(t) = f_1 a_1(0) + f_2 a_2(0) + f_3 a_1^\dagger(0) + f_4 a_2^\dagger(0),$$
$$a_2(t) = h_1 a_1(0) + h_2 a_2(0) + h_3 a_1^\dagger(0) + h_4 a_2^\dagger(0), \quad (3)$$

where f_i and h_i are functions of time. Therefore, the Hamiltonian and hence the temporal evolution of a_1 and a_2 are known if the parameters f_i and h_i are evaluated. The detailed solution is already available in our recent publication [24,25]. Unfortunately, the exact analytical closed form solution for f_i and h_i are unavailable. Therefore, an approximate solution

is found useful for investigating the dynamics of the present non-degenerate parametric oscillator. In order to do so, we use the so-called short-time approximation and hence the solution assumes the following form:

$$f_1(t) = \mathrm{e}^{-i\Omega_1 t} + \left(8ig^2\Omega_2\frac{t^3}{3!} + 16g^2\Omega_1\Omega_2\frac{t^4}{4!} + \cdots\right). \tag{4}$$

The terms proportional to gt, g^2t^2 etc. increase indefinitely with the increase of time t, and hence these terms are called 'secular terms'. As a consequence, the analytical solution for $f_1(t)$ diverges as the time progresses indefinitely. These secular terms pose serious difficulty and are inevitable in perturbative solutions to the coupled nonlinear differential equations. Of course, the secular terms are not harmful if we keep ourselves confined for small-time t. Barring the condition of small t, the secular terms are also tackled by various methods. These include multiscale perturbation theory [26–28], tucking-in technique etc. [29]. In the present investigation, we basically give a flavour of the tucking-in technique devised by Bellman [29]. In the light of the tucking-in technique, we express $f_1(t)$ in a compact form

$$f_1(t) \simeq \mathrm{e}^{-i\Omega_1 t}\cosh gt - (\cosh gt - 1) \times \left[1 - \frac{8}{3}(\mathrm{e}^{-i\Omega_1 t} - 1) - \frac{8}{3}(\mathrm{e}^{i\Omega_3 t} - 1)\right]. \tag{5}$$

Of course, in deriving eq. (5), we have neglected the terms beyond second orders in interaction constant (i.e. g^2t^2). Knowing the solution for $f_1(t)$, we now calculate the remaining $f_i(t)$. Now, with the application of tucking-in technique [29], the analytical expressions for f_2, f_3 and f_4 assume the following form:

$$f_2(t) \simeq 2i\sin gt\,\mathrm{e}^{(-i\Omega_3 t)/2}, \tag{6}$$

$$f_3(t) \simeq \frac{4g^2t^2}{3}(\mathrm{e}^{-i\Omega_2 t} - 1) \tag{7}$$

and

$$f_4(t) \simeq -i\sinh gt\,\mathrm{e}^{-i\Omega_1 t}(1 + \mathrm{e}^{i\Omega_3 t}). \tag{8}$$

Before we go further, we give a critical comparison of f_i's with those of their counterparts under tucked-in conditions. These are shown in figure 2. We observe a reasonable agreement between them. Before we go further, we calculate the commutation relation of the solution of the annihilation operator involving the signal field (3) and its Hermitian conjugates. Therefore, we have

$$[a_1(t),\ a_1^\dagger(t)] = [a_1(0),\ a_1^\dagger(0)] = 1, \tag{9}$$

where the analytical expressions for f_i are used. The equal time commutation relation (9) authenticates the validity of solution (3). The identical reasoning is valid for the idler mode as well. Depending upon the nonlinear constant, it is possible to have the dimensionless interaction constant as positive and negative. It is clear that parameters f_1 and f_3 involving eqs (4) and (7) respectively are even functions of dimensionless interaction constant gt up to the significant orders. On the other hand, parameters f_2 and f_4 involving eqs (6) and (8) are odd functions of gt. Now, evaluation of h_i's are being made as well. These are given by

$$h_1(t) \simeq 2i\sin gt\,\mathrm{e}^{(-i\Omega_3 t)/2}, \tag{10}$$

$$h_2(t) \simeq \mathrm{e}^{-i\Omega_2 t}\cosh gt - (\cosh gt - 1) \times \left[1 - \frac{8}{3}(\mathrm{e}^{-i\Omega_2 t} - 1) - \frac{8}{3}(\mathrm{e}^{i\Omega_3 t} - 1)\right] \tag{11}$$

$$h_3(t) \simeq -i\sinh gt\,\mathrm{e}^{-i\Omega_2 t}(1 + \mathrm{e}^{i\Omega_3 t}) \tag{12}$$

$$h_4(t) \simeq \frac{4g^2t^2}{3}(\mathrm{e}^{-i\Omega_1 t} - 1). \tag{13}$$

It is found that the direct short-time solutions for signal and idler modes involving eq. (3) coincide exactly with those of the solutions available through eqs (8) and (9) where the so-called direct method is not used. The direct solutions of the signal and idler modes are certainly easier to get as long as we are interested in terms involving t^3. However, the terms beyond t^3 will be extremely complicated because they involve non-commuting operators. On the other hand, the indirect method of getting a short-time solution is much easier even if we keep the terms beyond t^4. In addition to this, there is a possibility of getting exact analytical solutions for parameters f_i's. Apart from the possibilities of getting exact analytical solutions of f_i's, the exact numerical solutions are quite achievable. However, we do not have any intention to investigate numerical solutions to the problem in the present paper. Therefore, the present approach enjoys more advantages than the so-called direct method.

3. The temporal evolution of useful operators

Now, we calculate the temporal evolution of a few useful operators. These operators will be used to calculate the quantum statistical properties of the radiation field. In order to do so, we express the temporal evolution of the photon number operators for signal ($\hat{n}_1 = a_1^\dagger a_1$) and idler ($\hat{n}_2 = a_2^\dagger a_2$) modes. These are given by

$$\begin{aligned} a_1^\dagger(t)a_1(t) = {} & (|f_1|^2 a_1^\dagger(0)a_1(0) + f_2 f_1^* a_1^\dagger(0)a_2(0) \\ & + f_1 f_2^* a_2^\dagger(0)a_1(0) + f_4 f_2^* a_2^{\dagger 2}(0) \\ & + f_2 f_4^* a_2^2(0) + f_3 f_1^* a_1^{\dagger 2}(0) + f_1 f_3^* a_1^2(0)) \\ & + |f_2|^2 a_2^\dagger(0)a_2(0) + |f_4|^2(1 + a_2^\dagger(0)a_2(0)) \end{aligned}$$

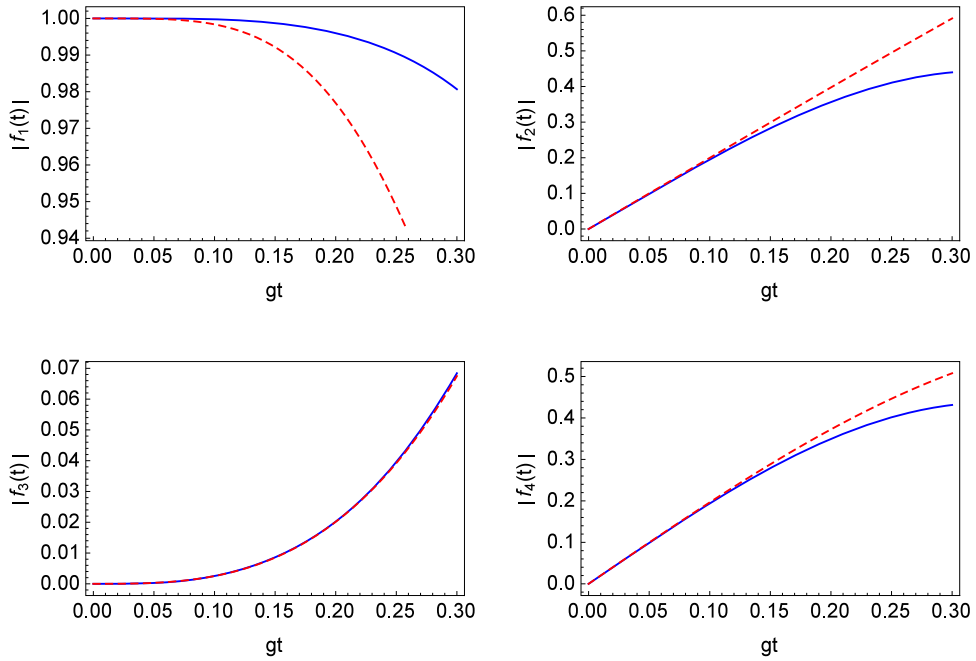

Figure 2. Plot of $|f_i(t)|$ as a function of dimensionless interaction constant gt for $\bar{n}_1(0) = 0$, $\bar{n}_2(0) = 0$, $\Omega_1 t = 2.0gt$ and $\Omega_2 t = 1.9gt$. The red and blue lines correspond to the situations with tucking-in and without tucking-in techniques.

$$
\begin{aligned}
&+f_1 f_4^* a_2(0)a_1(0) + f_4 f_1^* a_1^\dagger(0)a_2^\dagger(0) \quad (14)\\
a_2^\dagger(t)a_2(t) = {}& |h_2|^2 a_2^\dagger(0)a_2(0) + h_2 h_1^* a_1^\dagger(0)a_2(0)\\
&+h_1 h_2^* a_2^\dagger(0)a_1(0)\\
&+h_3 h_1^* a_1^{\dagger 2}(0) + h_1 h_3^* a_1^2(0)\\
&+h_4 h_2^* a_2^{\dagger 2}(0) + h_2 h_4^* a_2^2(0)\\
&+|h_1|^2 a_1^\dagger(0)a_1(0) + h_3 h_2^* a_2^\dagger(0)a_1^\dagger(0)\\
&+h_2 h_3^* a_1(0)a_2(0)\\
&+|h_3|^2(a_1^\dagger(0)a_1(0) + 1), \qquad (15)
\end{aligned}
$$

where the terms beyond g^2t^2 are neglected. Now, we calculate the square of the number operators for the signal and idler modes. These are given by

$$
\begin{aligned}
\hat{n_1^2}(t) = {}& |f_1|^2 a_1^\dagger(0)a_1(0)[|f_1|^2 a_1^\dagger(0)a_1(0)\\
&+f_2 f_1^* a_1^\dagger(0)a_2(0)\\
&+f_1 f_2^* a_2^\dagger(0)a_1(0) + f_3 f_1^* a_1^{\dagger 2}(0) + f_1 f_3^* a_1^2(0)\\
&+f_4 f_1^* a_1^\dagger(0)a_2^\dagger(0) + f_1 f_4^* a_2(0)a_1(0)\\
&+|f_4|^2 a_2(0)a_2^\dagger(0) + |f_2|^2 a_2^\dagger(0)a_2(0)\\
&+f_4 f_2^* a_2^{\dagger 2}(0) + f_2 f_4^* a_2^2(0)]\\
&+f_2 f_1^* a_1^\dagger(0)a_2(0)[(|f_1|^2 a_1^\dagger(0)a_1(0)\\
&+f_2 f_1^* a_1^\dagger(0)a_2(0) + f_1 f_2^* a_2^\dagger(0)a_1(0)\\
&+f_1 f_4^* a_2(0)a_1(0) + f_4 f_1^* a_1^\dagger(0)a_2^\dagger(0))]\\
&+f_1 f_2^* a_2^\dagger(0)a_1(0)[(|f_1|^2 a_1^\dagger(0)a_1(0)\\
&+f_2 f_1^* a_1^\dagger(0)a_2(0) + f_1 f_2^* a_2^\dagger(0)a_1(0)\\
&+f_1 f_4^* a_2(0)a_1(0) + f_4 f_1^* a_1^\dagger(0)a_2^\dagger(0))]\\
&+f_3 f_1^* |f_1|^2 a_1^{\dagger 3}(0)a_1(0)\\
&+f_1 f_3^* |f_1|^2 a_1^2(0)a_1^\dagger(0)a_1(0)\\
&+(|f_2|^2 a_2^\dagger(0)a_2(0) + f_4 f_2^* a_2^{\dagger 2}(0)\\
&+f_2 f_4^* a_2^2(0))|f_1|^2 a_1^\dagger(0)a_1(0)\\
&+(f_1 f_4^* a_2(0)a_1(0) + f_4 f_1^* a_1^\dagger(0)a_2^\dagger(0)\\
&+|f_4|^2 a_2(0)a_2^\dagger(0))|f_1|^2 a_1^\dagger(0)a_1(0)\\
&+(f_1 f_4^* a_2(0)a_1(0)\\
&+f_4 f_1^* a_1^\dagger(0)a_2^\dagger(0))(f_2 f_1^* a_1^\dagger(0)a_2(0)\\
&+f_1 f_2^* a_2^\dagger(0)a_1(0) + f_1 f_4^* a_2(0)a_1(0)\\
&+f_4 f_1^* a_1^\dagger(0)a_2^\dagger(0)) \qquad (16)\\
\hat{n_2^2}(t) = {}& |h_2|^2 a_2^\dagger(0)a_2(0)[|h_2|^2 a_2^\dagger(0)a_2(0)\\
&+h_2 h_1^* a_1^\dagger(0)a_2(0) + h_1 h_2^* a_2^\dagger(0)a_1(0)\\
&+h_3 h_1^* a_1^{\dagger 2}(0) + h_1 h_3^* a_1^2(0) + h_4 h_2^* a_2^{\dagger 2}(0)\\
&+h_2 h_4^* a_2^2(0) + |h_1|^2 a_1^\dagger(0)a_1(0)\\
&+h_3 h_2^* a_2^\dagger(0)a_1^\dagger(0) + h_2 h_3^* a_1(0)a_2(0)\\
&+|h_3|^2(a_1^\dagger(0)a_1(0) + 1)]\\
&+h_1 h_2^* a_2^\dagger(0)a_1(0)(|h_2|^2 a_2^\dagger(0)a_2(0)
\end{aligned}
$$

$$
\begin{aligned}
&+h_3h_2^*a_2^\dagger(0)a_1^\dagger(0) + h_2h_3^*a_1(0)a_2(0)\\
&+h_2h_1^*a_1^\dagger(0)a_2(0) + h_1h_2^*a_2^\dagger(0)a_1(0))\\
&+h_2h_1^*a_1^\dagger(0)a_2(0)(|h_2|^2a_2^\dagger(0)a_2(0)\\
&+h_3h_2^*a_2^\dagger(0)a_1^\dagger(0) + h_2h_3^*a_1(0)a_2(0)\\
&+h_2h_1^*a_1^\dagger(0)a_2(0) + h_1h_2^*a_2^\dagger(0)a_1(0))\\
&+(|h_1|^2a_1^\dagger(0)a_1(0) + h_3h_1^*a_1^{\dagger 2}(0)\\
&+h_1h_3^*a_1^2(0) + h_4h_2^*a_2^{\dagger 2}(0) + h_2h_4^*a_2^2(0)\\
&+|h_3|^2(a_1^\dagger(0)a_1(0)+1))|h_2|^2a_2^\dagger(0)a_2(0)\\
&+(h_3h_2^*a_2^\dagger(0)a_1^\dagger(0)\\
&+h_2h_3^*a_1(0)a_2(0))(|h_2|^2a_2^\dagger(0)a_2(0)\\
&+h_2h_1^*a_1^\dagger(0)a_2(0) + h_1h_2^*a_2^\dagger(0)a_1(0)\\
&+h_3h_2^*a_2^\dagger(0)a_1^\dagger(0) + h_2h_3^*a_1(0)a_2(0)). \qquad (17)
\end{aligned}
$$

The temporal evolution of the number operators (14) and (15) and the square of the number operators (16) and (17) are extremely useful for investigating various quantum statistical properties of the radiation field. These include squeezing [30,31], photon antibunching [3,31–33] and sub-Poissonian photon statistics [31,33]. The concept of antibunching is an interesting idea where the photons come singly (i.e. not in a bunch). This is contrary to the concept of photons in an incandescent light source from which the photons come together (i.e. bunch). There are several reports where the antibunching is substantiated by experimental observation.

4. Antibunching of photons: Results and discussions

In order to investigate the bunching and/or antibunching of photons from a light source, we need to calculate the second-order correlation (intensity correlation) function for zero time delay. Now, we know that the second-order correlation function for zero time delay is defined in the following manner [31–33]:

$$g_i^2(0) = \frac{\langle a_i^{\dagger 2}(t)a_i^2(t)\rangle}{\langle a_i^\dagger(t)a_i(t)\rangle^2}, \qquad (18)$$

where the subscripts $i = 1$ and 2 stand for the signal and idler modes respectively. We put eq. (18) in a more convenient form

$$g_i^2(0) - 1 = \frac{(\Delta n_i)^2 - \bar{n}_i}{\bar{n}_i^2} = \frac{D_i}{\bar{n}_i^2}, \qquad (19)$$

where $\bar{n}_i$ is the average number of photons in the field beyond interaction. The second-order variance $(\Delta n_i)^2$ involving the number operator is also essential for investigating the antibunching of photons. The numerator $D_i = (\Delta n_i)^2 - \bar{n}_i$ of the right hand of eq. (19) dictates the bunching and antibunching of photons as the denominator is positive definite. For example, for $D_i < 0$, the photons are antibunched because $g_i^2(0) < 1$. On the other hand, for $D_i = 0$ the photons are unbunched [3] and for $D_i > 0$ the photons are bunched. Therefore, to calculate various quantum statistical properties of the signal and idler modes, we need to specify the initial states of the said modes through which the average values of those operators are to be evaluated. There are a lot of possibilities for choosing the initial states. These include number states, coherent states, two-photon (squeezed) coherent states [34], binomial states [35], odd and even coherent states [36]. In the present investigation, however, we shall keep ourselves confined only with the number states and coherent states.

4.1 *Signal and idler modes are in number states*

Now, in terms of the initial number states, we calculate the average excitation (photon) number in the signal ($\bar{n}_1$) and idler ($\bar{n}_2$) modes. These are given by

$$\bar{n}_1(t) = |f_1|^2\bar{n}_1(0) + (|f_2|^2 + |f_4|^2)\bar{n}_2(0) + |f_4|^2 \qquad (20)$$

and

$$\bar{n}_2(t) = (|h_1|^2 + |h_3|^2)\bar{n}_1(0) + |h_2|^2\bar{n}_2(0) + |h_3|^2. \qquad (21)$$

For initial vacuum field (i.e. $\bar{n}_1(0) = 0 = \bar{n}_2(0)$), we obtain non-zero excitation in the signal and idler modes. The green curve in figure 3a shows that the number of photons in the signal mode reaches the value 0.2 from its initial value 0 for dimensionless interaction parameter $gt = 0.3$. Identical situation occurs for idler mode as well which is shown in figure 3b. Interestingly, the generation of the signal and idler photons out of the vacuum fields exhibit identical temporal evolution quantitatively and qualitatively as well because the pump photon is converted to signal and idler photons. The signal photon number and the idler photon numbers under the RWA are also exhibited (blue curves) in figures 3a and in 3b respectively. By analysing figures 3a and 3b, we observe that the differences between the values of the photon number without RWA (green curve) and with RWA (blue curve) are substantial as the dimensionless interaction time is increased. The direct numerical calculations of the coupled differential equations involving the signal and idler modes of Hamiltonian (1) are also obtained by using the QuTip3.1.0 [37,38]. These numerical solutions are exploited to obtain the temporal evolution of the signal and idler photons and are exhibited (dotted red points) in figures 3a and 3b. Interestingly, we obtain a

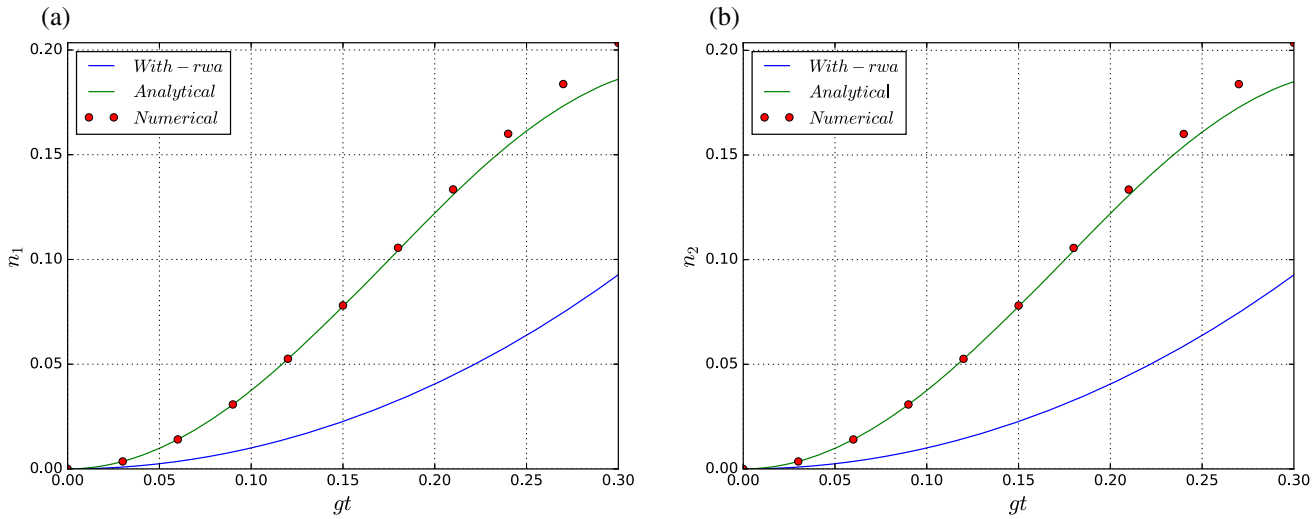

Figure 3. For the signal and idler in number states, the temporal evolution of signal (**a**) and idler (**b**) photons with (blue line) and without (green curves) RWA as function of gt for $\bar{n}_1(0) = 0$, $\bar{n}_2(0) = 0$, $\Omega_1 t = 2.0gt$ and $\Omega_2 t = 1.9gt$. The corresponding numerical results based on QuTip 3.1.0 are shown as red points in figures 3a and 3b. The approximate analytical results without RWA (green curves) coincide exactly with those of the direct numerical results corresponding to the red points.

perfect matching between the analytical and the numerical results. Of course, these exhibited results are for small values of dimensionless interaction time ($gt \ll 1$). Now, we calculate the average values of the square of the number operators involving signal and idler modes. These are given by

$$\begin{aligned}\bar{n}_1^2(t) = {} & |f_1|^4\bar{n}_1^2(0) + |f_1|^2|f_2|^2\,(4\bar{n}_1(0)\bar{n}_2(0) \\ & +\bar{n}_1(0) + \bar{n}_2(0)) \\ & +|f_1|^2|f_4|^2\,(4\bar{n}_1(0)\bar{n}_2(0) \\ & +3\bar{n}_1(0) + \bar{n}_2(0) + 1) \qquad (22)\\ \bar{n}_2^2(t) = {} & |h_2|^4\bar{n}_2^2(0) + |h_1|^2|h_2|^2\,(4\bar{n}_1(0)\bar{n}_2(0) \\ & +\bar{n}_1(0) + \bar{n}_2(0)) \\ & +|h_2|^2|h_3|^2\,(4\bar{n}_1(0)\bar{n}_2(0) \\ & +\bar{n}_1(0) + 3\bar{n}_2(0) + 1) \qquad (23)\end{aligned}$$

For the signal mode, we use eqs (20) and (22) for calculating the second-order correlation function for zero time delay available through eq. (19). We already mentioned that the numerator of eq. (19) is quite useful for investigating the antibunching of photons in the signal and idler modes. Hence, we have

$$\begin{aligned}D_1 = {} & |f_1|^2|f_2|^2\,(2\bar{n}_1(0)\bar{n}_2(0) + \bar{n}_1(0) + \bar{n}_2(0)) \\ & +|f_1|^2|f_4|^2\,(2\bar{n}_1(0)\bar{n}_2(0) + \bar{n}_1(0) + \bar{n}_2(0) + 1) \\ & -|f_1|^2\bar{n}_1(0) - \left(|f_2|^2 + |f_4|^2\right)\bar{n}_2(0) - |f_4|^2 \qquad (24)\end{aligned}$$

$$\begin{aligned}D_2 = {} & |h_1|^2|h_2|^2\,(2\bar{n}_1(0)\bar{n}_2(0) + \bar{n}_1(0) + \bar{n}_2(0)) \\ & +|h_2|^2|h_3|^2\,(2\bar{n}_1(0)\bar{n}_2(0) + \bar{n}_1(0) + \bar{n}_2(0) + 1) \\ & -\left(|h_1|^2 + |h_3|^2\right)\bar{n}_1(0) - |h_2|^2\bar{n}_2(0) - |h_3|^2. \qquad (25)\end{aligned}$$

Now, for single input we may assume that there is no idler photon at $t = 0$ (i.e. $\bar{n}_2(0) = 0$). Therefore, eqs (24) and (25) reduce to

$$D_1 = |f_1|^2(|f_2|^2 + |f_4|^2 - 1)\bar{n}_1(0) + |f_4|^2(|f_1|^2 - 1) \qquad (26)$$

$$\begin{aligned}D_2 = {} & |h_2|^2(|h_1|^2 + h_3|^2)\bar{n}_1(0) + |h_3|^2(|h_2|^2 - 1) \\ & -(|h_1|^2 + |h_3|^2)\bar{n}_1(0). \qquad (27)\end{aligned}$$

In order to investigate the antibunching of photons in the signal and idler modes, we calculate D_i for various physical situations which are exhibited in figures 4a–4d. For the vacuum signal field ($\bar{n}_1(0) = 0$), it is clear that the values of D_1 governed by eq. (26) are always negative for small interaction constant. Now, for $\bar{n}_1 = 1.0$ and $\bar{n}_2 = 2.0$, the parameter D_1 and hence the antibunching of signal mode with (without) RWA are shown using the blue (green) curve in figure 4a. The exact numerical solution under QuTip 3.1.0 is shown as red points in figure 4a. It is a matter of satisfaction that the analytical results coincide with the numerical one quite nicely. With the increase of the dimensionless interaction constant gt, the values of D_1 increases and hence the decrease of the antibunching effects (figure 4a). However, the effects of the increase of gt are not sensitive for the situation with RWA (blue curve). The antibunching effects of the idler mode shows identical behaviour with those of the signal mode and are exhibited in figure 4b. Now, with the increase of idler photons from $\bar{n}_2 = 1.0$ to $\bar{n}_2 = 3.0$, the antibunching effects of the signal and idler modes are reduced which are shown in figures 4c and 4d respectively. However, in all these situations, the coincidence of the analytical and numerical results are

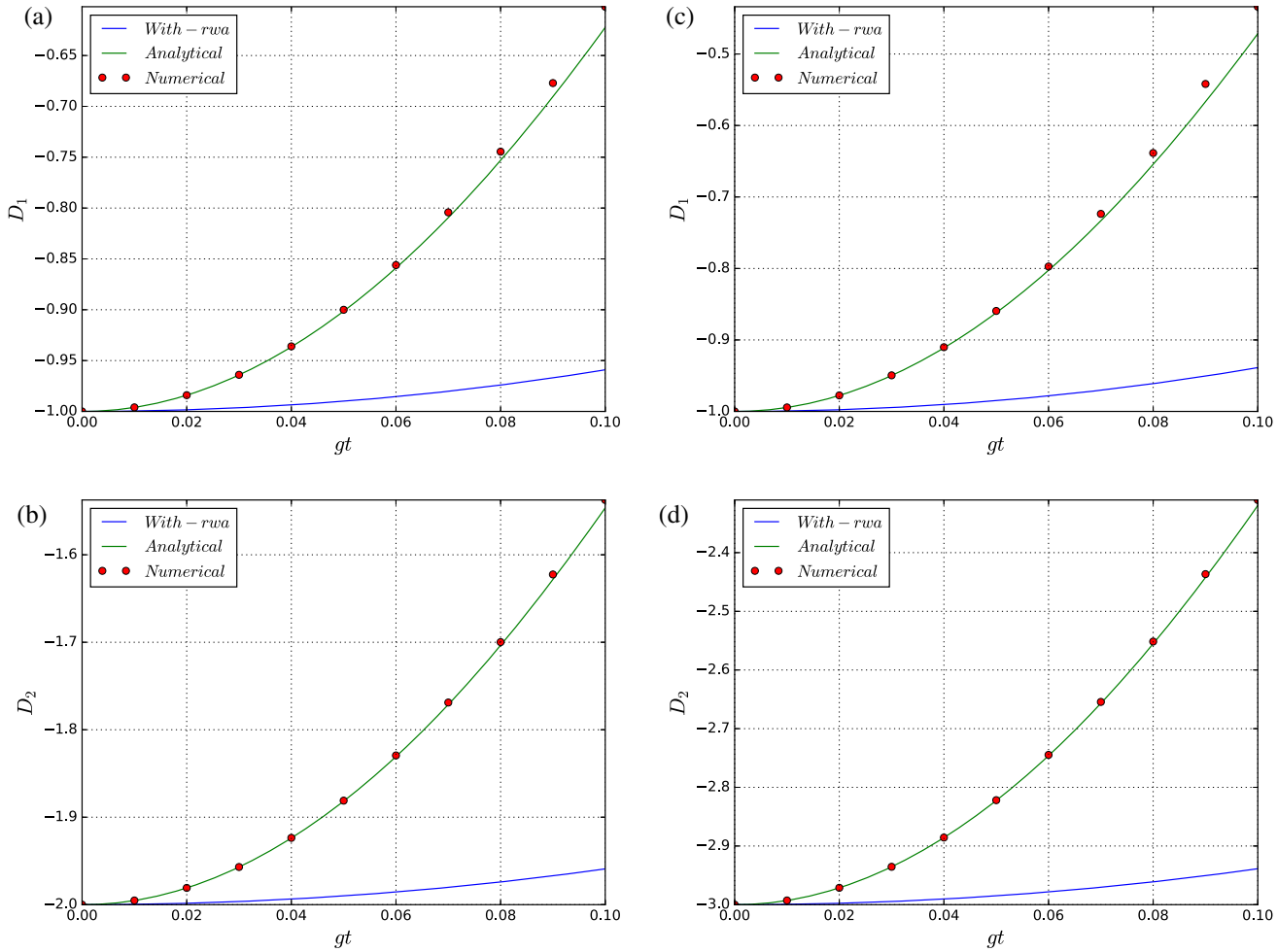

Figure 4. Plot of the parameters D_1 (eq. (26)) (**a**) and D_2 (eq. (27)) (**b**) as functions of the interaction constant gt for $\bar{n}_1(0) = 1.0$, $\bar{n}_2(0) = 2.0$, $\Omega_1 t = 2.0gt$ and $\Omega_2 t = 1.9gt$. In (**c**) and (**d**), the parameters D_1 and D_2 are plotted respectively for $\bar{n}_1(0) = 1.0$ and $\bar{n}_2(0) = 3.0$. The blue and green lines correspond to the situations with RWA and without RWA respectively. The corresponding numerical results based on QuTip 3.1.0 are shown as red points in figures 4a–4d. The approximate analytical results without RWA (green curves) coincide exactly with those of the direct numerical results corresponding to the red points.

quite satisfactory. Hence, at least for small interaction time gt, the signal photons are always antibunched for a non-degenerate parametric oscillator with the chaotic input radiation field. Interestingly, the signal field with zero signal photons exhibit antibunching effects in the signal mode. These are purely quantum optical phenomena as the photons are antibunched despite the absence of signal photons at $t = 0$. Therefore, we observe that the input chaotic signal field is unable to produce squeezing effects. However, it indeed produces antibunched light as output which is happened to be a purely quantum mechanical phenomenon. On the contrary, the use of RWA kills the contribution of f_2. The corresponding D_1 under RWA assumes the following condition:

$$D_1^{\mathrm{RWA}} = \bar{n}_1(0)\cosh^2 gt\left(\sinh^2 gt - 1\right) + \sinh^4 gt. \tag{28}$$

In case the signal and idler are prepared in the vacuum field, the antibunching of photons in the signal field under RWA is completely absent. These results are in sharp contrast when the RWA is not used. However, the antibunching of photons in the signal field is still possible (figures 4a and in 4c) for small interaction time gt provided $\bar{n}_1 \neq 0$.

4.2 *Signal and idler modes are in coherent state*

By assuming that the signal and idler modes are prepared in the initial coherent states, we investigate the quadrature fluctuations and the evolution of photon numbers in these modes. The initial composite coherent state for the signal and idler modes are assumed as $|\alpha\rangle = |\alpha_1, \alpha_2\rangle$. Now, the corresponding eigenvalue equation $a_i|\alpha\rangle = \alpha_i|\alpha\rangle$. The eigenvalue α_i is in general complex and $|\alpha_i|^2 = \bar{n}_i$ is the number of photons present

in the coherent field corresponding to $|\alpha_i\rangle$. Therefore, in terms of the initial composite coherent state, we calculate the average number of photons present in the signal $n_{1c}(t)$ and idler $n_{2c}(t)$. Therefore, we have

$$\begin{aligned} n_{1c}(t) &= |f_1|^2|\alpha_1|^2 + f_2 f_1^* \alpha_1^* \alpha_2 \\ &+ f_1 f_2^* \alpha_1 \alpha_2^* + f_3 f_1^* \alpha_1^{*2} + f_1 f_3^* \alpha_1^2 \\ &+ |f_2|^2|\alpha_2|^2 + f_4 f_2^* \alpha_2^{*2} \\ &+ f_2 f_4^* \alpha_2^2 + f_1 f_4^* \alpha_2 \alpha_1 \\ &+ f_4 f_1^* \alpha_1^* \alpha_2^* + |f_4|^2(|\alpha_2|^2 + 1), \end{aligned} \tag{29}$$

$$\begin{aligned} n_{2c}(t) &= |h_1|^2|\alpha_1|^2 + h_2 h_1^* \alpha_1^* \alpha_2 \\ &+ h_1 h_2^* \alpha_1 \alpha_2^* + h_3 h_1^* \alpha_1^{*2} \\ &+ h_1 h_3^* \alpha_1^2 + |h_2|^2|\alpha_2|^2 + h_4 h_2^* \alpha_2^{*2} \\ &+ h_2 h_3^* \alpha_1 \alpha_2 + h_3 h_2^* \alpha_1^* \alpha_2^* \\ &+ |h_3|^2(|\alpha_1|^2 + 1) + h_2 h_4^* \alpha_2^2, \end{aligned} \tag{30}$$

where subscript c stands for the average (expectation) values evaluated using the coherent state basis. The temporal evolution of the signal and idler photons for the initially prepared composite coherent state are shown in figures 5a and 5b respectively. The identical nature of the curves in figures 5a and 5b assert that they are created in an identical manner from the pump photon. Nevertheless, the numerical results under QuTip 3.1.0 for the signal and idler modes with initial composite coherent state are exhibited as the red dotted curves in figures 5a and 5b. The exact coincidence of the numerical results with those of the analytical one substantiates the validity of both the approaches. Now, the expectation values of the square of the photon number operators in terms of the initial coherent state are also calculated. These are

$$\begin{aligned} \bar{n}_{1c}^2(t) &= |f_1|^2[(|f_1|^2(|\alpha_1|^4 + |\alpha_1|^2) \\ &+ f_2 f_1^* \alpha_1^* \alpha_2(1 + |\alpha_1|^2) + f_1 f_2^* \alpha_1 \alpha_2^* |\alpha_1|^2 \\ &+ f_3 f_1^*(|\alpha_1|^2 + 2)\alpha_1^{*2} + f_1 f_3^* |\alpha_1|^2 \alpha_1^2) \\ &+ (|f_2|^2|\alpha_1|^2|\alpha_2|^2 + f_4 f_2^* |\alpha_1|^2 \alpha_2^{*2} \\ &+ f_2 f_4^* |\alpha_1|^2 \alpha_2^2) \\ &+ (f_1 f_4^* |\alpha_1|^2 \alpha_1 \alpha_2 + f_4 f_1^*(1 + |\alpha_1|^2)\alpha_1^* \alpha_2^* \\ &+ |f_4|^2|\alpha_1|^2(|\alpha_2|^2 + 1))] \\ &+ f_2 f_1^*[(|f_1|^2|\alpha_1|^2 \alpha_1^* \alpha_2 + f_2 f_1^* \alpha_1^{*2} \alpha_2^2 \\ &+ f_1 f_2^* |\alpha_1|^2(|\alpha_2|^2 + 1) \\ &+ f_1 f_4^* |\alpha_1|^2 \alpha_2^2 + f_4 f_1^* \alpha_1^{*2}(|\alpha_2|^2 + 1))] \\ &+ f_1 f_2^*[(|f_1|^2(1 + |\alpha_1|^2)\alpha_1 \alpha_2^* \\ &+ f_2 f_1^*(1 + |\alpha_1|^2)|\alpha_2|^2 \\ &+ f_1 f_2^* \alpha_1^2 \alpha_2^{*2} + f_1 f_4^* |\alpha_2|^2 \alpha_1^2 \\ &+ f_4 f_1^*(1 + |\alpha_1|^2)\alpha_2^{*2})] \\ &+ f_3 f_1^* |f_1|^2 |\alpha_1|^2 \alpha_1^{*2} \\ &+ f_1 f_3^* |f_1|^2(|\alpha_1|^2 + 2)\alpha_1^2(0) \\ &+ |f_1|^2(|f_2|^2|\alpha_1|^2|\alpha_2|^2 \\ &+ f_4 f_2^*| \\ &\alpha_1|^2 \alpha_2^{*2} + f_2 f_4^* |\alpha_1|^2 \alpha_2^2) \\ &+ (|f_1|^2 f_1 f_4^* \alpha_1 \alpha_2(1 + |\alpha_1|^2) \\ &+ |f_1|^2 f_4 f_1^* |\alpha_1|^2 \alpha_1^* \alpha_2^* \\ &+ |f_1|^2|f_4|^2|\alpha_1|^2(1 + |\alpha_2|^2)) \\ &+ f_1 f_4^*(f_2 f_1^* \alpha_2^2(1 + |\alpha_1|^2) \\ &+ f_1 f_2^* \alpha_1^2(1 + |\alpha_2|^2) + f_1 f_4^* \alpha_1^2 \alpha_2^2 \\ &+ f_4 f_1^*(1 + |\alpha_1|^2)(1 + |\alpha_2|^2)) \\ &+ f_4 f_1^*(f_2 f_1^* \alpha_1^{*2}|\alpha_2|^2 \\ &+ f_1 f_2^* \alpha_2^{*2}|\alpha_1|^2 \\ &+ f_1 f_4^* |\alpha_1|^2|\alpha_2|^2 + f_4 f_1^* \alpha_2^{*2} \alpha_1^{*2}) \end{aligned} \tag{31}$$

$$\begin{aligned} \bar{n}_{2c}^2(t) &= |h_2|^2[|h_2|^2(|\alpha_2|^4 + |\alpha_2|^2) \\ &+ h_2 h_1^* |\alpha_2|^2 \alpha_1^* \alpha_2 + h_1 h_2^* \alpha_1 \alpha_2^*(1 + |\alpha_2|^2) \\ &+ h_3 h_1^* \alpha_1^{*2}|\alpha_2|^2 + h_1 h_3^* \alpha_1^2 |\alpha_2|^2 \\ &+ |h_1|^2|\alpha_1|^2|\alpha_2|^2 \\ &+ h_4 h_2^*(\alpha_2^{*2}|\alpha_2|^2 + 2\alpha_2^{*2}) + h_2 h_4^* \alpha_2^2 |\alpha_2|^2 \\ &+ h_3 h_2^* \alpha_1^* \alpha_2^*(1 + |\alpha_2|^2) + h_2 h_3^* \alpha_1 \alpha_2 |\alpha_2|^2 \\ &+ |h_3|^2|\alpha_2|^2(|\alpha_1|^2 + 1)] \\ &+ h_1 h_2^*(|h_2|^2 \alpha_1 \alpha_2^*|\alpha_2|^2 \\ &+ h_3 h_2^* \alpha_2^{*2}(|\alpha_1|^2 + 1) + h_2 h_3^* \alpha_1^2 |\alpha_2|^2 \\ &+ h_2 h_1^* |\alpha_2|^2(|\alpha_1|^2 + 1) + h_1 h_2^* \alpha_2^{*2} \alpha_1^2) \\ &+ h_2 h_1^*(|h_2|^2 \alpha_1^* \alpha_2(1 + |\alpha_2|^2) \\ &+ h_3 h_2^* \alpha_1^{*2}(1 + |\alpha_2|^2) + h_2 h_3^* \alpha_2^2 |\alpha_1|^2 \\ &+ h_2 h_1^* \alpha_1^{*2} \alpha_2^2 + h_1 h_2^* |\alpha_1|^2(|\alpha_2|^2 + 1)) \\ &+ |h_2|^2(|h_1|^2|\alpha_1|^2|\alpha_2|^2 + h_3 h_1^* \alpha_1^{*2}|\alpha_2|^2 \\ &+ h_1 h_3^* \alpha_1^2 |\alpha_2|^2 + h_4 h_2^* \alpha_2^{*2}|\alpha_2|^2 \\ &+ h_2 h_4^*(||\alpha_2|^2 + 2)\alpha_2^2 \\ &+ |h_3|^2|\alpha_2|^2(|\alpha_1|^2 + 1)) \\ &+ h_3 h_2^*(|h_2|^2 \alpha_1^* \alpha_2^*|\alpha_2|^2 + h_2 h_1^* \alpha_1^{*2}|\alpha_2|^2 \\ &+ h_1 h_2^* \alpha_2^{*2}|\alpha_1|^2 \\ &+ h_3 h_2^* \alpha_1^{*2} \alpha_2^{*2} + h_2 h_3^* |\alpha_1|^2|\alpha_2|^2) \\ &+ h_2 h_3^*(|h_2|^2 \alpha_1 \alpha_2(1 + |\alpha_2|^2) \\ &+ h_2 h_1^* \alpha_2^2(1 + |\alpha_1|^2) \\ &+ h_1 h_2^* \alpha_1^2(1 + |\alpha_2|^2) \\ &+ h_3 h_2^*(|\alpha_1|^2 + 1)(|\alpha_2|^2 + 1) \\ &+ h_2 h_3^* \alpha_1^2 \alpha_2^2). \end{aligned} \tag{32}$$

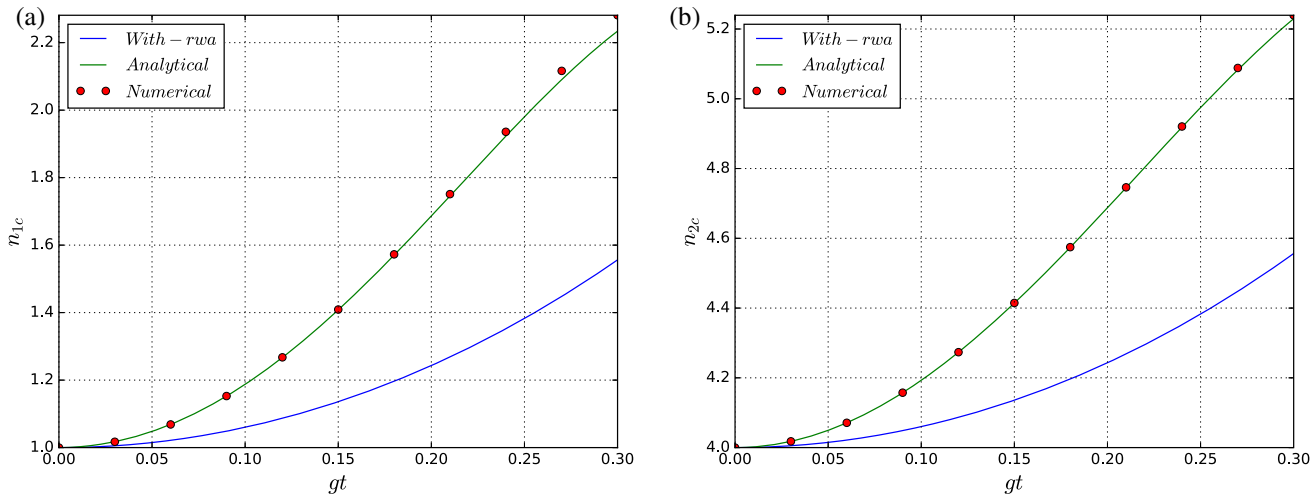

Figure 5. For the signal and idler in composite coherent states, the temporal evolution of signal (**a**) and idler (**b**) photons with (blue line) and without (green curves) RWA as a function of gt with $|\alpha| = 1$, $|\beta| = 2$, $\Omega_1 t = 2.0gt$ and $\Omega_2 t = 1.9gt$. The corresponding numerical results based on QuTip 3.1.0 are shown as red points in figures 5a and 5b. The approximate analytical results without RWA (green curves) coincide exactly with those of the direct numerical results corresponding to the red points.

Now, the second-order variances of the number operators involving the signal and idler modes follow immediately. These are given by

$$\begin{aligned}\Delta n_{1c}^2(t) = {} & |f_1|^2[|f_1|^2|\alpha_1|^2 + f_2 f_1^*|f_1|^2\alpha_1^*\alpha_2 \\ & +2f_3 f_1^*|f_1|^2\alpha_1^{*2} + f_4 f_1^*\alpha_1^*\alpha_2^*] \\ & +f_2 f_1^*[f_1 f_2^*|\alpha_1|^2 + f_4 f_1^*\alpha_1^{*2}] \\ & +f_1 f_2^*[|f_1|^2\alpha_1\alpha_2^* + f_2 f_1^*|\alpha_2|^2 \\ & +f_4 f_1^*\alpha_2^{*2}] \\ & +2f_1 f_3^*|f_1|^2\alpha_1^2 + |f_1|^2 f_1 f_4^*\alpha_1\alpha_2 \\ & +f_1 f_4^*(f_2 f_1^*\alpha_2^2 + f_1 f_2^*\alpha_1^2 \\ & +f_4 f_1^*(1 + |\alpha_1|^2 + |\alpha_2|^2)) \end{aligned} \tag{33}$$

and

$$\begin{aligned}\Delta n_{2c}^2(t) = {} & |h_2|^2[|h_2|^2|\alpha_2|^2 + h_1 h_2^*\alpha_1\alpha_2^* \\ & +2h_4 h_2^*\alpha_2^{*2} + h_3 h_2^*\alpha_1^*\alpha_2^*] \\ & +h_2 h_1^*(|h_2|^2\alpha_1^*\alpha_2 \\ & +h_3 h_2^*\alpha_1^{*2} + h_1 h_2^*|\alpha_1|^2) \\ & +h_1 h_2^*(h_3 h_2^*\alpha_2^{*2} + h_2 h_1^*|\alpha_2|^2) \\ & +h_2 h_3^*(|h_2|^2\alpha_1\alpha_2 + h_2 h_1^*\alpha_2^2 \\ & +h_1 h_2^*\alpha_1^2 + h_3 h_2^*(|\alpha_1|^2 + |\alpha_2|^2 + 1)) \\ & +2|h_2|^2 h_2 h_4^*\alpha_2^2 \end{aligned} \tag{34}$$

Now, we assume the case of a single input (i.e. the idler photon is zero initially). Therefore, the corresponding D for the signal and idler modes follow as

$$\begin{aligned} D_{1c}(t) = {} & |f_1|^4|\alpha_1|^2 + 2f_3 f_1^*|f_1|^2\alpha_1^{*2} \\ & +2f_1 f_3^*|f_1|^2\alpha_1^2 + f_1^2 f_2^* f_4^*\alpha_1^2 \\ & +f_2 f_4 f_1^{*2}\alpha_1^{*2} + |f_1|^2|f_2|^2|\alpha_1|^2 \\ & +|f_4|^2|f_1|^2(1 + |\alpha_1|^2) \\ & -(|f_1|^2|\alpha_1|^2 + f_3 f_1^*\alpha_1^{*2} \\ & +f_1 f_3^*\alpha_1^2 + |f_4|^2) \end{aligned} \tag{35}$$

and

$$\begin{aligned} D_{2c}(t) = {} & h_1^* h_3(|h_2|^2 - 1)\alpha_1^{*2} + h_1 h_3^*(|h_2|^2 - 1)\alpha_1^2 \\ & +|h_1|^2|h_2|^2|\alpha_1|^2 \\ & +|h_3|^2(|h_2|^2 - 1)(|\alpha_1|^2 + 1). \end{aligned} \tag{36}$$

For the signal vacuum field, eqs (35) and (36) reduce to the following form:

$$D_{1c}(t) = |f_4|^2(|f_1|^2 - 1) \tag{37}$$

and

$$D_{2c}(t) = |h_3|^2(|h_2|^2 - 1). \tag{38}$$

Finally, eqs (37) and (38) are plotted as functions of interaction time in figures 6a and 6b respectively. Both the parameters D_{1c} and D_{2c} involving the signal and idler fields respectively go below zero (i.e. negative) as indicated in figures 6a and 6b respectively. Hence, for the initial vacuum fields for the signal and idler modes, we obtain the effects of photon antibunching at least for small dimensionless interaction time gt. These results are opposite to the results obtained under RWA because, the use of RWA will give $|f_1|^2 = 1$ and $|h_2|^2 = 1$ and hence the right-hand side of both eqs (37) and (38) would vanish. Hence, the possibilities of antibunching of photons are washed out if we do not go beyond RWA.

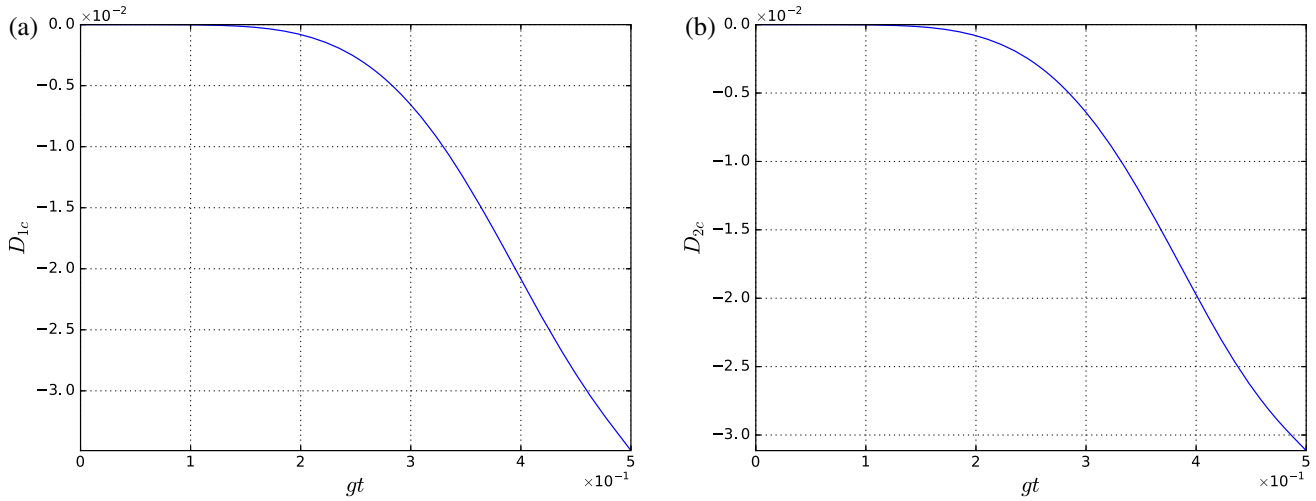

Figure 6. The parameter D_{1c} (eq. (37)) and D_{2c} (eq. (38)) are plotted as a function of dimensionless interaction constant gt for $|\alpha_1|^2 = 0$, $|\alpha_2|^2 = 0$, $\Omega_1 t = 1.8gt$ and $\Omega_2 t = 1.7gt$.

The purpose of the article is certainly to emphasise the usefulness of analytical solutions for investigating the antibunching of photons of radiation fields coupled to the NDPO. We remain unsuccessful in providing exact analytical solutions of the nonlinear coupled differential equations involving non-commuting field operators. Instead, we obtain approximate solutions to the field operators involving the signal and idler fields of NDPO beyond RWA. The analytical results are based on the small dimensionless interaction time. In order to provide acceptability of the solutions, we provide the numerical solutions based on QuTip3.1.0. It is a matter of satisfaction that the approximate analytical solutions and hence the calculated parameters involving the antibunching of photons corroborates the results obtained by the numerical one. Of course, the matching of these results are exhibited for small interaction constant where the analytical solutions hold good.

5. Conclusion

The problem of a non-degenerate parametric oscillator (NDPO) is quite attractive because of its potential applications in producing correlated photons and hence in the application of quantum information theory. The NDPO involves the second-order nonlinear medium and hence it is easier to achieve it experimentally compared to those of the nonlinear phenomena/devices involving higher orders of nonlinearities. The NDPO is a text book problem when the pump is taken as a strong one. A large variety of applications and the possible generations of parametric oscillators are discussed in a recent review [12]. Of course, the solutions and hence the quantum dynamics of a NDPO is certainly non-trivial because they involve coupled nonlinear differential equations. However, under the usual RWA, the NDPO offers exact analytical solutions and hence the quantum dynamics. Now, the use of RWA eliminates some small interesting effects for example, the Bloch–Siegert (B–S) effect. Interestingly, the B–S effect is well known and is substantiated experimentally for the low-frequency (NMR) region [14]. In addition to this, the use of RWA for the calculation of Berry's phase leads to incorrect results [15]. Because of the recent developments in the field of ultra-strongly and deep-strongly coupling in the matter–field interaction, we find that the use of RWA is highly undesirable and lead to incorrect results. Therefore, it is highly desirable to investigate the solutions and hence the quantum dynamics of NDPO beyond RWA. The model calculation of NDPO in the present article is relevant in the context of boson–boson coupling and quantum stimulators [39]. Keeping these facts in mind, the solutions of the NDPO beyond the RWA are used to investigate the non-classical properties (antibunching of photons) of the thermal and coherent light coupled to it. The squeezing, higher-ordered squeezing and mixed-mode squeezing are already investigated in the same model of NDPO [24]. We got some interesting results involving the squeezing [24] and photon antibunching of the input radiation field coupled to the NDPO which are not available when the RWA is used. For example, under the realm of RWA, the squeezing effects of the signal/idler modes of the NDPO are completely absent for input radiation field prepared in the number state. It is also established that the antibunching of photons for the initial vacuum fields prepared in the coherent states is impossible if the RWA is used. Therefore, the solutions of NDPO beyond RWA give rise to some interesting results involving squeezing and antibunching of photons. However, the presence of secular terms

in the solutions is certainly a non-trivial problem. The secular terms can be tackled by several methods. We, however, use the tucking-in techniques to avoid the secular nature of the analytical solutions. Interestingly, we got a fair agreement between the solutions of f_i and its tucked-in counterparts. In addition to this, the solution under short time has its problems. In these investigations, however, the approximate analytical solutions of the NDPO are used. Therefore, it will be an interesting problem to check the suitability/validity of the available results [24] involving squeezing, higher order squeezing and mixed mode squeezing for field operators with the numerical results under QuTip 3.1.0. However, we do not have any intention to substantiate the earlier results by using the numerical technique. In figures 3a and 3b, the temporal evolution of the signal and idler photons are calculated numerically by using QuTip 3.1.0 and exhibited (red dots). The same numerical method is exploited to calculate the parameters $D_1(D_2)$ involving the antibunching of signal (idler) photons and are shown as red dots in figures 5a and 5b. Interestingly, we obtain the exact coincidence of the numerical results with those of the analytical one beyond RWA. These results substantiate the validity of both the results. In spite of the shortcomings of the solutions beyond RWA, we believe that these solutions will be acceptable for investigating several other non-classical properties of the NDPO.

Acknowledgements

Generous funding from the Malaysia Ministry of Education FRGS17-024-0590 is gratefully acknowledged. One of the authors (SM) thanks the University Grants Commission, New Delhi for financial support through a major research project (F.No.42-852/2013(SR)). SM also is thankful to the Council of Scientific and Industrial Research (CSIR), Government of India for financial support (03(1283)/13/EMR-II). MK is grateful to the UGC for the award of senior research fellowship (F1-17.1/2016-17/NFST-2015-17-ST-WES-878/(SA-III/Website).

References

[1] R W Boyd, *Nonlinear optics,* 2nd edn (Academic Press, New York, 2006).
[2] A Yariv, *Quantum electronics,* 3rd edn (John Wiley & Sons, New York, 1988)
[3] J Perina, Z Hradil and J Branislav, *Quantum optics and fundamentals of physics* (Kluwer Academic Publishers, Dordrecht, 1994)
[4] Z Ficek and M R B Wahiddin, *Quantum optics: Fundamentals and applications* (International Islamic University Malaysia, Kuala Lumpur, 2004)
[5] Z Ficek and M R B Wahiddin, *Quantum optics for beginners* (Pan Stanford Publishing, Singapore, 2014)
[6] P A Franken, A E Hills, C W Peters and G Weinreich, *Phys. Rev. Lett.* **7**, 118 (1961)
[7] D R White and W H Louisell, *Phys. Rev. A* **1**, 1347 (1970)
[8] A Yariv and W H Louisell, *IEEE J. Quant. Electron.* **QE-2**, 418 (1966)
[9] L-A Wu, M Xiao and H J Kimble, *J. Opt. Soc. Am. B* **10**, 1465 (1987)
[10] N Bloembergen and Y R Shen, *Phys. Rev. A* **133**, 37 (1964).
[11] W H Louisell, A Yariv and A E Siegman, *Phys. Rev.* **124**, 1646 (1961)
[12] Y Zhang, *Fron. Phys. China* **3**, 126 (2008)
[13] N C Wong, *Phys. Rev. A* **45**, 3176 (1992)
[14] L Allen and J H Eberly, *Optical resonance and two-level atoms* (Dover Publications, New York, 1987)
[15] J Larson, *Phys. Rev. Lett.* **108**, 033601 (2012)
[16] M Janowicz and A Orlowski, *Rep. Math. Phys.* **54**, 71 (2004)
[17] M Mirzaee and M Batavani, *Chin. Phys. B* **24**, 040306 (2015)
[18] A Moroz, *Ann. Phys.* **340**, 252 (2014)
[19] F Yoshihara, T Fuse, S Ashhab, K Kakuyanagi, S Saito and K Semba, *Nat. Phys.* **13**, 44 (2017)
[20] A Le Boite, M-J Hwang, H Nha and M B Plenio, *Phys. Rev. A* **94**, 033827 (2016)
[21] P Forn-Díaz, J J García-Ripoll, B Peropadre, J-L Orgiazzi, M A Yurtalan, R Belyansky, C M Wilson and A Lupascu, *Nat. Phys.* **13**, 39 (2017)
[22] C Ciuti, G Bastard and I Carusotto, *Phys. Rev. B* **72**, 115303 (2005)
[23] C Ciuti and I Carusotto, *Phys. Rev. A* **74**, 033811 (2006)
[24] M Alam, S Mandal and M R B Wahiddin, *Optik* **157**, 1035 (2018)
[25] M Alam, S Mandal and M R B Wahiddin, *Opt. Commun.* **398**, 1 (2017)
[26] A H Nayfeh, *Introduction to perturbation techniques* (Wiley, New York, 1981)
[27] A H Nayfeh and D T Mook, *Non-linear oscillations* (Wiley, New York, 1979)
[28] C M Bender and L M A Bettencourt, *Phys. Rev. Lett.* **77**, 4114 (1996)
[29] R Bellman, *Methods of nonlinear analysis* (Academic Press, New York, 1970) Vol. 1, p. 198
[30] D F Walls, *Nature* **306**, 141 (1983)
[31] R Loudon and P L Knight, *J. Mod. Opt.* **34**, 709 (1987)
[32] D F Walls, *Nature* **280**, 451 (1979)
[33] R Loudon, *The quantum theory of light*, 2nd edn (Oxford University Press, Oxford, 1983)
[34] H P Yuen, *Phys. Rev. A* **13**, 2226 (1976)
[35] D Stoller, B E A Saleh and M C Teich, *Opt. Acta* **32**, 345 (1985)
[36] C C Gerry, *J. Mod. Opt.* **40**, 1053 (1993)

[37] J R Johansson, P D Nation and F Nori, *Comput. Phys. Commun.* **184**, 1234 (2013)
[38] J R Johansson, P D Nation and F Nori, *Comput. Phys. Commun.* **183**, 1760 (2012)
[39] S Fedortchenko, S Felicetti, D Markovic, S Jezouin, A Keller, T Coudreau, B Huard and P Milman, 1612.05542v1